Building a mathematical model describing the dome profile of a solid fuel engine case made from composite materials using winding technology

Tran Ngoc Thanh, Dinh Van Hien, Bui Van Am*

Institute of Missile, Academy of Military Science and Technology, 17 Hoang Sam, Nghia Do, Hanoi, Vietnam.

*Corresponding author: kimam1994offich@gmail.com

Received 9 Sep. 2025; Revised 20 Nov. 2025; Accepted 10 Feb. 2026; Published 25 Feb. 2026.

DOI: https://doi.org/10.54939/1859-1043.j.mst.109.2026.146-153

ABSTRACT

With the advantage of high specific strength, composite materials are the first choice for manufacturing a solid fuel engine case to increase the engine's stuffing coefficient. The main problem for designing an engine case from composite materials is the problem of determining the dome profile of the engine case. To determine the dome profile based on continuum theory, the article focuses on building a general mathematical model describing the dome profile of the case with an internal thermal protection layer under internal pressure p and axial force. Using this mathematical model, the influence of axial force and nozzle radius on the dome profile of the engine case is analyzed. The results of the article are the basis for designing the case of a solid fuel engine from composite materials.

Keywords: Solid fuel engine case made from composite material; Dome profile; Axial force; Nozzle radius.

1. INTRODUCTION

Research on the design and manufacture of a solid fuel engine (SFE) case from composite materials using winding technology has been of interest to many scientists in the world and has achieved quite a lot of success. Typically, the case of the 115Д367 engine is made from fibreglass, the case of the Crotale-NG missile is made from T-40 carbon fiber [10], etc. However, research documents on the design of SFE cases from composite materials are almost secret, accessible documents are mainly about the theory of winding pressure cylindrical vessel in p with a dome from composite materials with a shape similar to the SFE case.

For the design of the SPE case from composite materials, the problem of determining the dome profile is the most important. To determine the shape of the dome of the winding composite vessel, people approach it in two directions: the direction of netting theory and continuum theory. Netting theory is a theory that considers composite materials as unidirectional, where the stress in the fiber is evenly distributed along the fiber axis, and the same in all fibers. In the remaining theoretical direction, the composite material is a homogeneous material with anisotropic elasticity, meaning that the load-bearing capacity of the composite is not only considered along the fiber axis but also in the direction transverse to the fiber axis. Research on netting theory is summarized in many documents, typically the book of Vasiliev (2009) [9]. Based on the continuum theory, the publications of Liang et al. (2002) [2], based on geodesic roving trajectories; Vasiliev (2003) [8], Zu et al. (2010) [6], based on non-geodesic roving trajectories. In Viet Nam, research on the design of the SFE case has not really received much attention, research is mainly on rotating composite cylindrical shells, typically in projects [3].

In fact, the composite cylindrical vessel subjected to pressure in p has many differences compared to the SFE case from composite materials. The SFE case is subjected not only to internal pressure p but also to an axial force N caused by the inertial force during the movement. Under the effect of axial force N and pressure p, the internal force in the dome of the case changes differently from that of the pressure vessel, leading to changes in the mathematical model of stress-deformation in the case. From there, the mathematical model describing the dome profile of the

SFE case from composite materials changes compared to the mathematical model of the pressure vessel. In terms of structure, the dome of the SFE case has an open-polar hole shape connected to the ignition device or nozzle, while the pressure vessel has a dome sealed at both ends. In the case where the dome is connected to a nozzle, a part of the polar hole will be covered by the flange that still bears the pressure p. As a result, the force distribution at the polar hole q is changed depending on the nozzle radius, affecting the dome profile of the SFE case.

With the goal based on continuum theories to design the SFE case, the authors focus on building a general mathematical model to determine the dome profile of the SFE case made from a composite based on the geodesic and the non-geodesic roving trajectories. On that basis, analyze the influence of axial force and nozzle radius on the dome profile of the SFE case.

2. PROBLEM

2.1. Assumptions and geometrical-physical characteristics of the SFE case's dome

During engine operation, the SFE case is subjected to various loads, including mechanical and thermal loads. In the study, when we design the dome profile of the SFE case, the following assumptions are used:

- The pressure p inside the engine is a uniform pressure;

- When the engine is working, the case is subjected to a constant axial force N, which is equal to the maximum axial force acting on it.

- For composite materials used in the aerospace industry, the glass transition temperature of the resin is typically in the range of T_g = 200 - 260°C [1]. Under short-term thermal exposure with temperature $T \le 0,5T_g$, the mechanical properties of the fiber direction exhibit negligible variation [5]. According to the literature [4, 7], when designing a SFE case of composite materials, a sufficiently thick thermal protection layer is applied so that the casing temperature $T \le 0,5T_g$. Since the thermal effects are significantly smaller than the effects of pressure loading, the SFE case is designed using a safety factor instead of accounting directly for thermal stresses. Specifically, the design pressure is defined as $p = kp_{max}$, where $k = 2 - 3$ is safety factor [4] and p_{max} is the maximum internal pressure within the engine.

Consider a composite dome of the SFE case connected to the nozzle with a fiber (or a fiber tape) placed on the surface described in the polar coordinate system (z, r, θ), subjected to internal pressure p and axial force N as shown in figure 1. Some geometrical and physical characteristics of the SFE case related to this study are as follows:

- R, r_p are the radius of the cylindrical part and the radius of the dome hole, r_l is the inner radius of the nozzle, r_l = 0 if the SFE case is connected with the igniter.

- β is the winding angle, which is the angle formed by the tangent of the fiber trajectory with the tangent of the shell meridian;

- T_1 is the internal force in the meridian direction, T_2 is the internal force in the parallel direction, R_1 is the meridional radius, R_2 is the parallel radius.

- p is the calculated pressure in the engine, N is the axial force, and q is the force distribution at the polar hole [11].

$$q = \frac{pr_p}{2}\left(1 - \frac{r_l^2}{r_p^2}\right) \quad (1)$$

To build a mathematical equation describing the dome profile of the SFE case, it is necessary to solve the following problems:

- The winding problem is ensuring that the filament does not slip on the surface of the winding mandrel.

- Problems related to the equilibrium of internal forces in the dome of the SFE case.

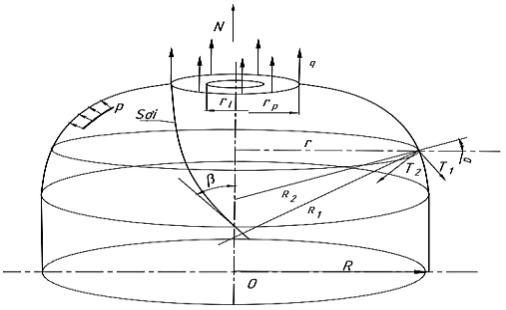

Figure 1. *The geometry of a dome profile of the SFE case.*

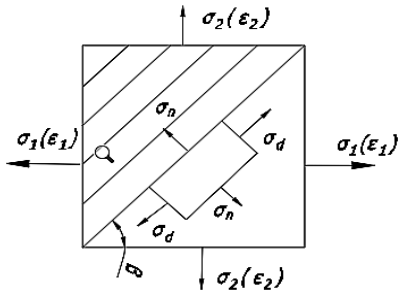

Figure 2. *Stress-strain components in the case's element.*

2.2. Non-slippage condition of the fiber

For the wound dome of the SFE case based on non-geodesic roving trajectories, according to [5], the non-geodesic wound trajectory equation is as follows:

$$\beta' = \frac{d\beta}{dz} = \lambda.(\frac{\sin\beta.\tan\beta}{r} - \frac{r".\cos\beta}{1+r'^2}) - \frac{r'.\tan\beta}{r} \tag{2}$$

where β' is the first derivative of β with respect to z, λ is the slip coefficient, which describes the slip tendency of the fiber, $r^{'}, r^{"}$ are first and second derivatives of r with respect to z.

Rearranging equation (2) we obtain:

$$\lambda = \frac{\sqrt{1+r'^2}.(r'.\sin\beta + r.\beta'.\cos\beta)}{\sqrt{1+r'^2}.\sin^2\beta - r.r".\cos^2\beta} \tag{3}$$

To prevent the fiber from slipping, the fiber's slip coefficient must be ensured [5]:

$$\lambda \le [\lambda] \tag{4}$$

where $[\lambda]$ is the allowable slip coefficient.

For the wound dome of the SFE case based on geodesic roving trajectories, the fiber has no tendency to slip, meaning that $\lambda = 0$ the geodesic fiber trajectory equation becomes as follows:

$$r.\cos\beta = const \tag{5}$$

2.3. Equilibrium of internal forces in the dome of the SFE case

- *Internal force in the dome of the case*: Under the effect of pressure *p* and axial force *N,* internal force components appear as the meridional force T_1 and the parallel force T_2 [11]*:*

$$T_1 = \frac{pR_2}{2}(1 - \frac{r_l^2}{r^2} + \frac{N}{\pi r^2 p}) \tag{6}$$

$$T_2 = \frac{pR_2}{2}\left(2 - \frac{R_2}{R_1}(1 - \frac{r_l^2}{r^2} + \frac{N}{\pi r^2 p})\right) \tag{7}$$

The average stresses in the meridional and parallel directions can be determined:

$$\sigma_1 = T_1 / h \tag{8}$$

$$\sigma_2 = T_2 / h \tag{9}$$

where *h* is the thickness of the SFE case's dome.

- *Internal force in the SFE case's dome is generated by pressure p and axial force N*: Describe the stress components in the dome element of the case as shown in figure 2.

Because the dome case has a symmetrical shape with the axial direction coinciding with the direction of the composite material, the stress and shear strain components are zero [11]. According to the mechanical theory of composite materials [11], the stress and strain in the case have the following relationship:

$$\sigma_1 = \sigma_d.\cos^2\beta + \sigma_n.\sin^2\beta \quad (10)$$

$$\sigma_2 = \sigma_d.\sin^2\beta + \sigma_n.\cos^2\beta \quad (11)$$

$$\varepsilon_1 = \frac{\varepsilon_n.\sin^2\beta - \varepsilon_d.\cos^2\beta}{\sin^4\beta - \cos^4\beta} \quad (12)$$

$$\varepsilon_2 = \frac{\varepsilon_d.\sin^2\beta - \varepsilon_n.\cos^2\beta}{\sin^4\beta - \cos^4\beta} \quad (13)$$

$$\varepsilon_d = \frac{\sigma_d}{E_d} - \frac{\nu_{dn}}{E_n}.\sigma_n \quad (14)$$

$$\varepsilon_n = \frac{\sigma_n}{E_n} - \frac{\nu_{nd}}{E_d}.\sigma_d \quad (15)$$

$$E_d.\nu_{dn} = E_n.\nu_{nd} \quad (16)$$

where σ_d, σ_n, ε_d, ε_n are the stress and strain in the direction longitudinal and transverse to the fiber axis; E_d, E_n, ν_{dn}, ν_{nd} are the elastic modulus and Poisson's ratio of the composite material in the longitudinal and transverse directions.

Substitute equations (12-16) into equations (10-11) to obtain the equations:

$$\sigma_1 = A_{11}.\varepsilon_1 + A_{12}.\varepsilon_2 \quad (17)$$

$$\sigma_2 = A_{21}.\varepsilon_1 + A_{22}.\varepsilon_2 \quad (18)$$

where:

$$A_{11} = \frac{E_d}{1-\nu_{dn}\nu_{nd}}.\cos^4\beta + 2\frac{E_d}{1-\nu_{dn}\nu_{nd}}.\nu_{dn}.\sin^2\beta.\cos^2\beta + \frac{E_n}{1-\nu_{nd}\nu_{dn}}.\sin^4\beta$$

$$A_{12} = A_{21} = (\frac{E_d}{1-\nu_{dn}\nu_{nd}} + \frac{En}{1-\nu_{nd}\nu_{dn}}).\cos^2\beta.\sin^2\beta + \frac{E_d}{1-\nu_{dn}\nu_{nd}}.\nu_{dn}(\sin^4\beta + \cos^4\beta)$$

$$A_{22} = \frac{E_d}{1-\nu_{dn}\nu_{nd}}.\sin^4\beta + 2\frac{E_d}{1-\nu_{dn}\nu_{nd}}.\nu_{dn}.\sin^2\beta.\cos^2\beta + \frac{E_n}{1-\nu_{dn}\nu_{nd}}.\cos^4\beta$$

Consider this ratio σ_2/σ_1, from (6), (7), (10) and (11) we have:

$$\frac{\sigma_2}{\sigma_1} = \frac{\tan^2\beta + k}{1 + k.\tan^2\beta} = \left(\frac{2}{1 - \frac{r_l^2}{r^2} + \frac{N}{\pi r^2 p}} + \frac{r.r^{"}}{1 + r'^2} \right) \quad (19)$$

where $k = \sigma_n/\sigma_d$ is the stress ratio that characterizes the anisotropy of composite materials.

2.4. Minimum strain energy condition

According to the plasticity condition, the material energy changes from elastic to plastic state when the shape change potential energy (strain energy) reaches a certain value. Thus, if the strain energy is minimum, the load-bearing capacity of the structure is better. From this point of view, the minimum strain energy condition is used to design the optimal dome of the SFE case.

The deformation energy of the case element is determined as follows:

$$U = \frac{1}{2}\left(\varepsilon_1.\sigma_1 + \varepsilon_2.\sigma_2\right) \tag{20}$$

Set $\varphi = \sigma_1 / \sigma_2$, substitute equations (17), (18) into equation (20), we obtain:

$$U = \frac{\sigma_1^2}{2}.\frac{A_{22} - 2.\varphi.A_{12} + \varphi^2.A_{11}}{A_{22}.A_{11} - A_{12}^2} \tag{21}$$

To find the minimum of the function U, we use the Lagrange extremum method by considering the function:

$$f(A_{11}, A_{12}, A_{22}) = \frac{\sigma_1^2}{2}.\frac{A_{22} - 2\varphi.A_{12} + \varphi^2.A_{11}}{A_{22}.A_{11} - A_{12}^2} + \eta.\left[A - (A_{11} + 2.A_{12} + A_{22})\right] \tag{22}$$

where η is the parameter Lagrange. We have:

$$A_{11} + 2.A_{12} + A_{22} = A = const \tag{23}$$

According to the Lagrange extremum condition, the function f reaches a minimum when:

$$\frac{\partial f}{\partial A_{11}} = 0,\ \frac{\partial f}{\partial A_{22}} = 0,\ \frac{\partial f}{\partial A_{12}} = 0 \tag{24}$$

Solving (24) with constraint (23), we obtain $\varphi = (A_{22} + A_{12}) / (A_{11} + A_{12})$. Divide equation (17) by equation (18), we obtain:

$$\frac{\varepsilon_1}{\varepsilon_2} = \frac{\varphi.A_{22} - A_{12}}{A_{11} - \varphi.A_{12}} \tag{25}$$

Subtracting equation (25) by 1, we obtain:

$$\varepsilon_1 = \varepsilon_2 = \varepsilon = \frac{\sigma_1}{A_{11} + A_{12}} \tag{26}$$

2.5. Equations for determining the dome of the SFE case

Since $\varepsilon_1 = \varepsilon_2$, from (11) and (13) we have $\varepsilon_d = \varepsilon_n$. Combining (13), (14) and (15), we obtain:

$$k = \frac{\sigma_n}{\sigma_d} = \frac{E_n(1 + v_{nd})}{E_d(1 + v_{dn})} = const \tag{27}$$

From equations (19) and (27), we get the equations describing the dome profile of the SFE case:

$$r'' = \left(\frac{\tan^2\beta + k}{1 + k\tan^2\beta} - \frac{2.r^2}{r^2 - C_p.r_p^2 + C_n}\right)\frac{1 + r'^2}{r} \tag{28}$$

where $C_p = \left(\frac{r_l}{r_p}\right)^2$ - Coefficient nozzle radius, $C_n = \frac{N}{\pi R^2 p}$ - Axial force coefficient.

Converting equation (28) into non-dimensional form by placing $\bar{r} = r / R, \bar{z} = z / R$ and combining with equation (2), we get a system of equations describing the wound dome profile of the SFE case based on the non-geodesic roving trajectories and the continuum theory:

$$\begin{cases} \bar{r}'' = \left(\dfrac{\tan^2\beta + k}{1 + k\tan^2\beta} - \dfrac{2.\bar{r}^{-2}}{\bar{r}^{-2} - C_p.\bar{r}_p^{-2} + C_n} \right) \dfrac{1 + \bar{r}'^2}{\bar{r}} \\ \beta' = \lambda.\left(\dfrac{\sin\beta.\tan\beta}{\bar{r}} - \dfrac{\bar{r}''.\cos\beta}{1 + \bar{r}'^2} \right) - \dfrac{\bar{r}'.\tan\beta}{\bar{r}} \end{cases} \quad (29)$$

Combining equation (5) and the first equation of system (29), we get the system of equations describing the wound dome profile of the SFE case based on the continuum theory and geodesic roving trajectories. When the value of the anisotropy coefficient is k=0 in equation (29), we obtain the system of equations describing the wound dome profile of the SFE case based on the non-geodesic trajectories and the netting theory. The boundary conditions to solve the system of equations are $\bar{z}(0) = 0, \bar{r}(0) = 1, \bar{r}'(0) = 0, \beta(0) = \beta_{xd}$, where β_{xd} - Winding angle at the equator.

3. RESULTS AND DISCUSSION

3.1. Effect of axial force on the dome profile of the SFE

Figures 3, 4, 5, 6 show the influence of the coefficient C_n on the shape of the dome profile of the SFE. It can be seen that when the coefficient C_n increases, or the axial force N increases, to ensure the balance of the dome of the SFE, it tends to lengthen (the dome height z increases). However, when the axial force value increases too high, the dome of the SFE is bent and does not converge to the polar hole. The wound dome profile of the SFE case based on the geodesic roving trajectory tends to bend earlier than that dome based on the non-geodesic roving trajectory when having the same polar hole radius and coefficient *Cp*.

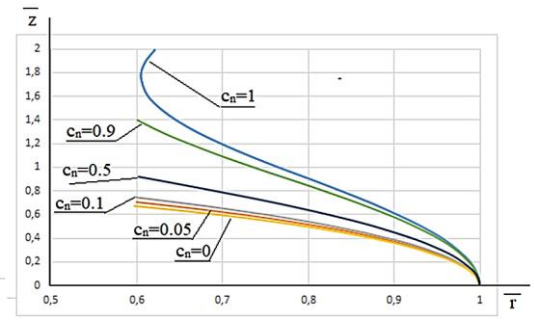

Figure 3. *Non-geodetic winding dome profile of the SFE with coefficient C_p= 0.5, $\bar{r}_p$ = 0.6.*

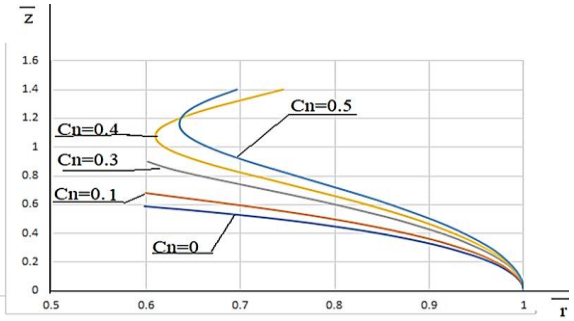

Figure 4. *Geodetic winding dome profile of the SFE with coefficient C_p= 0.5, $\bar{r}_p$ = 0.6.*

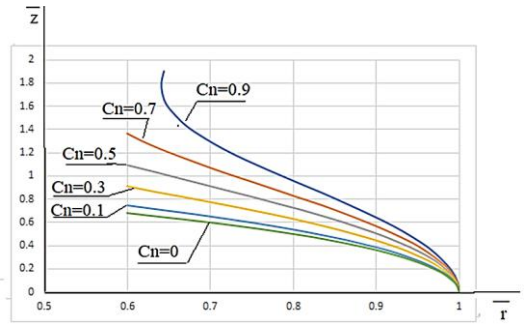

Figure 5. *Non-geodetic winding dome profile of the SFE with coefficient C_p= 0, $\bar{r}_p$ = 0.6.*

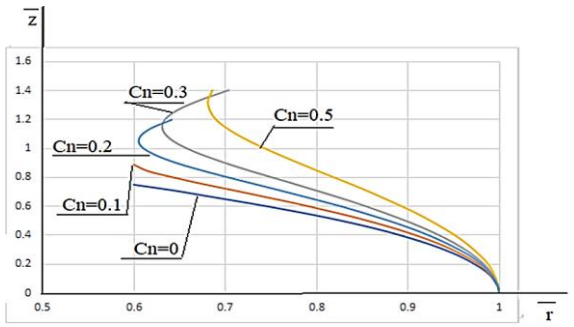

Figure 6. *Geodetic winding dome profile of the SFE with coefficient C_p= 0, $\bar{r}_p$ = 0.6.*

To overcome the phenomenon of the dome profile not converging towards the polar hole, it is necessary to use a convex curve with a radial radius of the correction point $r_f \geq r_i$. To overcome this, according to [6], a correction equation needs to be used, which has the form of equation (30).

$$\begin{cases} \left(\bar{z} + \bar{R}_{1f}.\sin\alpha_f - \bar{z}_f\right)^2 + \left(\bar{r} + \bar{R}_{1f}.\cos\alpha_f - \bar{r}_f\right)^2 = \bar{R}_{1f}^2 \\ \alpha_f = \text{acos}\left((1+\bar{r}^2)^{-1/2}\right)\Big|_{\bar{z}=\bar{z}_f} \end{cases} \tag{30}$$

where index f denotes the correction point; R_1 is the radius of the meridian arc at the correction point.

3.2. Effect of nozzle radius on the dome profile and the dome deformation of the SFE case

Figure 7 shows the dome deformation curve of the non-geodetic winding SFE case with different polar hole radii. When the polar hole radius increases, the forces in the meridian and parallel directions decrease, so to ensure the stable equilibrium of the dome, the dome height decreases. Figure 8 shows the dome deformation of the SFE case using carbon fiber composite material with epoxy resin under the pressure p = 24 MPa, coefficient C_n = 0.1. It can be seen that when the nozzle radius increases, the dome deformation gradually decreases due to the increase in the distribution force at the polar hole when the polar hole radius decreases. The largest deformation of the dome at the equatorial position gradually decreases as the radius decreases and there is a jump at the position near the polar hole.

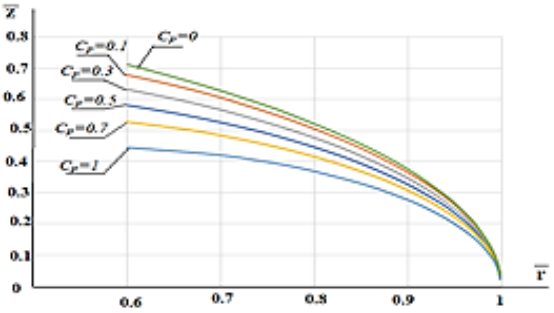

Figure 7. *Effect of nozzle radius on the dome profile of the SFE with coefficient Cp = 0.5, $\bar{r}_p$ = 0.6.*

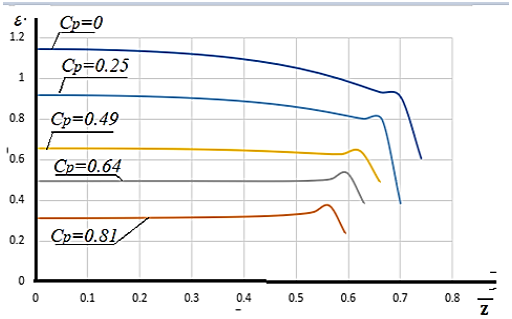

Figure 8. *Effect of nozzle radius on the dome deformation of the SFE case.*

4. CONCLUSIONS

Based on the continuum theory, the geometry and bearing characteristics of the SFE case were analyzed according to the proposed assumptions. Using the minimum deformation energy condition, a mathematical model was built to describe the dome profile of the SFE case under the influence of pressure p and axial force N, based on both geodesic and non-geodesic roving trajectories. From the mathematical model, the influence of axial force and nozzle radius on the dome profile of the SFE case was presented, and the following main points were drawn:

- When the axial force increases, the tendency of the dome profile of the SFE case not converge toward the polar hole increases. From there, a correction curve is proposed for the dome part, not converging toward the polar hole.

- When the polar hole radius increases, the height of the dome and the dome deformation of the SFE case both decrease due to the decrease in force q at the polar hole location.

REFERENCES

[1]. Agarwal, B. D.; Broutman, L. J.; Chandrashekhara, K., *"Analysis and Performance of Fiber Composites"*, Wiley, New Jersey, (2006).

[2]. Liang, C. C.; et al., *"Optimum design of dome contour for filament-wound composite pressure vessels based on a shape factor"*, Composite Structures, Vol. 58, No. 4, pp. 469–482, (2002).
[3]. Hien, D. V.; Thanh, T. N.; et al., *"Design of planar wound composite vessel based on preventing slippage tendency of fibers"*, Composite Structures, Vol. 254, Article 112820, (2020).
[4]. Milligan, D. J.; Ghoshal, A., *"Design and Analysis of a Composite-Lined Rocket Motor Case"*, NASA Technical Memorandum 107523, NASA Langley Research Center, Hampton, VA, (1992).
[5]. Wen, J.; Wu, Y., *"Effect of high temperature on mechanical properties and porosity of carbon fiber/epoxy composites"*, Composite Structures, Vol. 262, Article 113640, (2021).
[6]. Zu, L.; et al., *"Design of filament-wound domes based on continuum theory and non-geodesic roving trajectories"*, Composites Part A, Vol. 41, pp. 1312–1320, (2010).
[7]. U.S. Department of Defense, *"MIL-HDBK-17-1F: Composite Materials Handbook, Volume 1 – Polymer Matrix Composites Guidelines for Characterization of Structural Materials"*, Department of Defense, Washington, D.C., (2002).
[8]. Vasiliev, V. V.; Krikanov, A. A., *"New generation of filament-wound composite pressure vessels for commercial applications"*, Composite Structures, Vol. 62, No. 3, pp. 449–459, (2003).
[9]. Vasiliev, V. V., *"Composite Pressure Vessels: Analysis, Design, and Manufacturing"*, Bull Ridge Publishing, Blacksburg, Virginia, USA, (2009).
[10]. Калинчев, В. А.; Ягодников, Д. А., *"Технология производства ракетных двигателей твердого топлива"*, Технологии ракетно-космического машиностроения, Vol. 688, Moscow, (2010).
[11]. Буланов, И. М.; Смыслов, В. И.; Комков, М. А.; Кузнецов, В. И., *"Сосуды давления из композиционных материалов в конструкциях летательных аппаратов"*, Moscow, (1985).

TÓM TẮT

Xây dựng mô hình toán mô tả biên dạng đáy thân vỏ động cơ nhiên liệu rắn từ vật liệu composite theo công nghệ quấn

Để tăng hệ số nhồi cho động cơ, vật liệu composite là lựa chọn hàng đầu để chế tạo thân vỏ động cơ nhiên liệu rắn giúp tăng hệ số nhồi động cơ. Bài toán chính để thiết kế thân vỏ động cơ nhiên liệu rắn từ vật liệu composite là bài toán xác định biên dạng đáy thân vỏ động. Với mục tiêu xác định biên dạng đáy, bài báo trọng tâm xây dựng mô hình toán tổng quát mô tả biên đạng đáy thân vỏ động cơ có lớp bảo vệ nhiệt bên trong chịu áp lực trong p và lực dọc trục N. Dựa trên mô hình toán, phân tích sự ảnh hưởng lực dọc trục và bán kính loa phụt đến biên dạng đáy thân vỏ động cơ. Kết quả bài báo là cơ sở cho tính toán thiết kế thân vỏ động cơ nhiên liệu rắn từ vật liệu composite.

Từ khoá: Thân vỏ động cơ nhiên liệu rắn từ vật liệu composite; Biên dạng đáy thân vỏ; Lực dọc trục; Bán kính loa phụt.